POTENTIAL DIRECTIONS FOR THE USE OF QUANTUM COMPUTING IN CAA

Hans A. Kösel* and **Roland Ewert***

*Institute of Aerodynamics and Flow Technology, German Aerospace Center (DLR),
Lilienthalplatz 7, 38108 Braunschweig, Germany

10 October 2025,

1st International Conference on Applied Quantum Methods
in Computational Science and Engineering (AQMCSE)

DLR
Quantum Computing
Initiative
ToQuaFlics

DLR

Outline

1. Requirements for CAA and their Relation to Quantum Computing
2. A Quantum Algorithm for the Inhomogeneous Poisson Equation for Free Field Conditions
3. Preliminary Consideration on Computational Resources

Computational Aeroacoustics (CAA)

Aeroacoustics

sound generation in flows

- inherently due to turbulence
- fluid-structure interaction, e.g., propeller or vibration
-

sound propagation in flows

can be in complex geometries
→ e.g., effects like scattering or refraction

sound-flow interaction

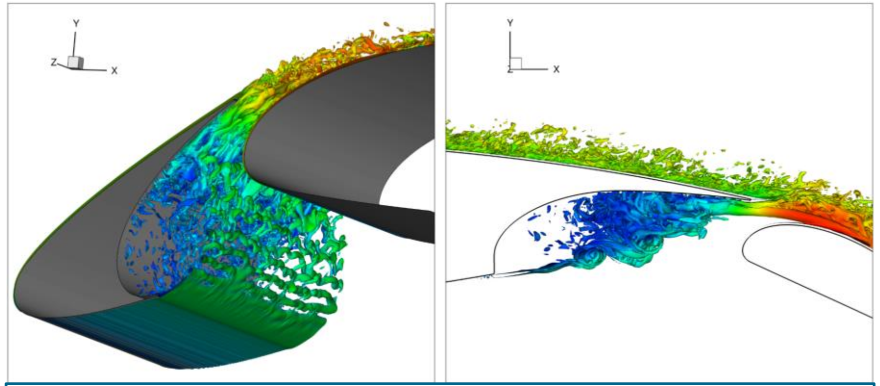

Instantaneous flow in slat and flap cove represented with the iso-surface of the vorticity magnitude, coloured with the velocity magnitude.

M. Soni et al., 28th AIAA/CEAS Aeroacoustics Conference, June 14 - 17 2022, Southampton, UK

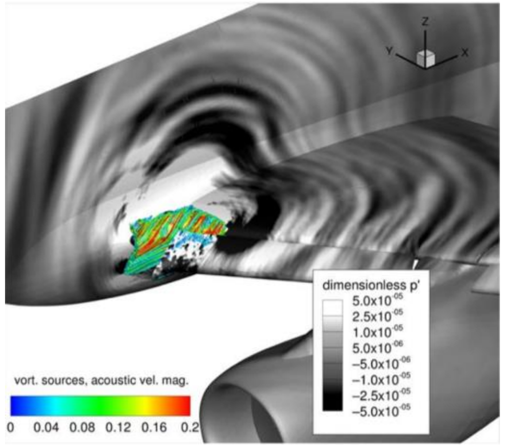

Instantaneous acoustic pressure and iso-surface of the vorticity.

S. Proskurov et al., *Airframe noise simulation of an A320 aircraft in landing configuration*, CEAS Aeronautical Journal (2025)

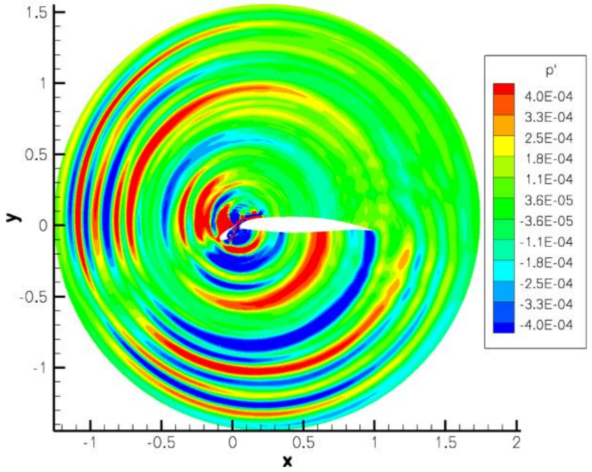

Pressure perturbation field.

M. Bauer et al., 15th AIAA/CEAS Aeroacoustics Conference, 11 - 13 May 2009, Miami, Florida, USA

State of the CAA Art

- currently managable at the DLR department ‘Technical Acoustics‘:

simulation property	order of magnitude
number of grid points	10^9
highest resolved frequency	10^4 Hz
simulated time	1 s

→ requires ‘time-marching‘ with a corresponding read out rate for the flow quantities, e.g., done with the lattice Boltzmann method (LBM)

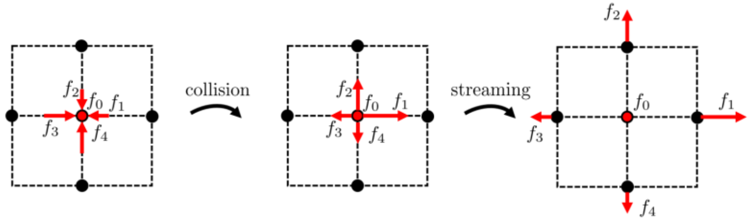

Implementation of a time step via collision step and streaming step as separate operations.
S. Kocherla et al., AVS Quantum Sci. **6**, 033806 (2024)

→ Can steps of such time-marching algorithms for CAA be accelerated via quantum computing (QC)?

Linear Operations

- often sufficient description of aeroacoustic problems via linear eqs.

  ‘*Quantum computers are naturally adept at performing linear operations* […]’

  Z. Holmes et al., Phys. Rev. Research **5**, 013105 (2023)

  → theoretically fewer computation steps, e.g., for

  - Fourier transformation (FT) via the QFT

    M. A. Nielsen and I. L. Chuang, *Quantum Computation and Quantum Information*, (10th anniversary edition, Cambridge University Press, 2010)

  - solving systems of linear eqs. via the HHL algorithm

    A. W. Harrow et al., Phys. Rev. Lett. **103**, 150502 (2009)

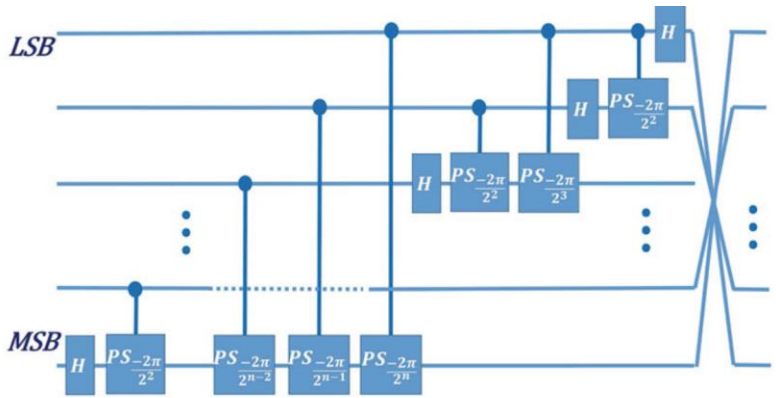

n-qubit QFT circuit.

H. Y. Wong, *Introduction to Quantum Computing* (2nd edition, Springer, 2023)

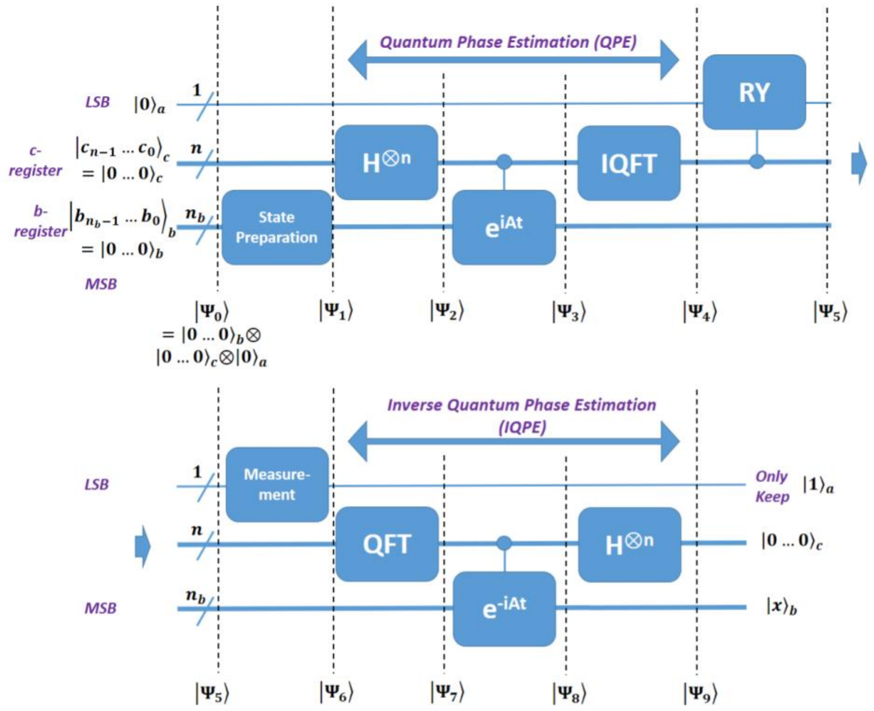

Workflow of the HHL algorithm.

A. Zaman et al., IEEE Access 11, pp. 77117-77131 (2023)

Linear Differential Equations in Aeroacoustics

- FT for solving **Poisson and wave eqs.**, e.g., for the Navier-Stokes eqs. for incompressible flow

$$\underline{\nabla} \cdot \underline{u} = 0, \qquad \frac{\partial}{\partial t}\underline{u} + \underline{u} \cdot \underline{\nabla u} + \frac{1}{\rho_0}\underline{\nabla} p = D\underline{\nabla}^2 \underline{u} \quad \Rightarrow \quad \underline{\nabla}^2 p = -\rho_0 \underline{\nabla} \cdot (\underline{u} \cdot \underline{\nabla u})$$

or also $\frac{\partial}{\partial t}\underline{\omega} + \underline{u} \cdot \underline{\nabla \omega} = D\underline{\nabla}^2 \underline{\omega}, \quad \underline{\omega} = \underline{\nabla} \times \underline{u}$

with $\underline{\nabla}^2 \underline{A} = -\underline{\omega}, \quad \underline{u} = \underline{\nabla} \times \underline{A}$ for 2D

- solving a system of linear eqs., e.g., in the **boundary element method (BEM)**
  → involves no time-marching

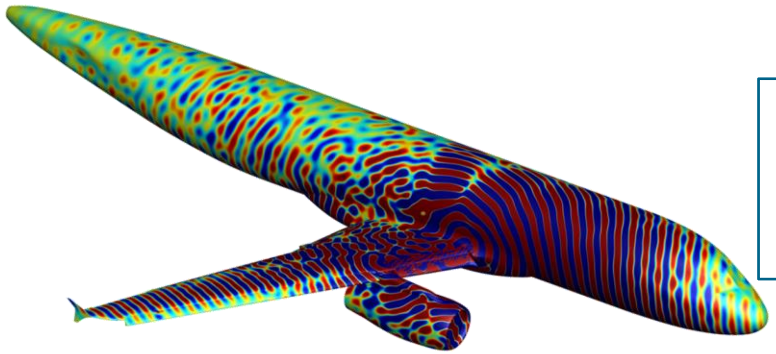

Simulation result of a FM-BEM procedure (FMCAS) used at the DLR department ‘Technical Acoustics‘.

Solution Approach

used FT convention:

$$\hat{f}(k_{x_i}) = \int_{-\infty}^{+\infty} f(x_i) e^{\mathrm{i}k_{x_i}x_i}\, dx_i \quad \Leftrightarrow \quad f(x_i) = \frac{1}{2\pi}\int_{-\infty}^{+\infty} \hat{f}(k_{x_i}) e^{-\mathrm{i}k_{x_i}x_i}\, dk_{x_i}, \quad x_i \in \{x, y, \dots\} \quad \Rightarrow \quad \frac{\partial}{\partial x_i} \longrightarrow -\mathrm{i}k_{x_i}$$

$$\nabla^2 \varphi(\underline{x}) = S(\underline{x})$$

FT of the given $S(\underline{x})$ ← implementable via the QFT

$$-\underline{k}^2 \hat{\varphi}(\underline{k}) = \hat{S}(\underline{k})$$

multiplication of $\hat{S}(\underline{k})$ by $-\frac{1}{\underline{k}^2}$

corresponds to a multiplication of the state vector by a corresponding diagonal matrix:

$$\frac{-1}{k_x^2 + k_y^2} \cdot \hat{S}(k_x, k_y)$$

$$\widehat{=} \begin{pmatrix} \frac{-1}{k_{x_1}^2 + k_{y_1}^2} & 0 & 0 & \dots & 0 \\ 0 & \frac{-1}{k_{x_2}^2 + k_{y_1}^2} & 0 & \dots & 0 \\ 0 & 0 & \ddots & & \vdots \\ \vdots & \vdots & & & \\ 0 & 0 & \dots & & \frac{-1}{k_{x_{N_x}}^2 + k_{y_{N_y}}^2} \end{pmatrix} \cdot \begin{pmatrix} \hat{S}(k_{x_1}, k_{y_1}) \\ \hat{S}(k_{x_2}, k_{y_1}) \\ \vdots \\ \hat{S}(k_{x_{N_x}}, k_{y_{N_y}}) \end{pmatrix}$$

→ implementable via the linear combination of unitary matrices (LCU method)

$$\hat{\varphi}(\underline{k}) = -\frac{\hat{S}(\underline{k})}{\underline{k}^2}$$

inverse FT of the expression for $\hat{\varphi}(\underline{k})$ ← implementable via the QFT

$$\varphi(\underline{x})$$

Multi-dimensional QFT

P. Pfeffer, arXiv:2301.13835v1 [quant-ph] (2023)

→ parallel implementation of the DFT of an amplitude encoded field $S(\underline{x})$

least significant bit (LSB)

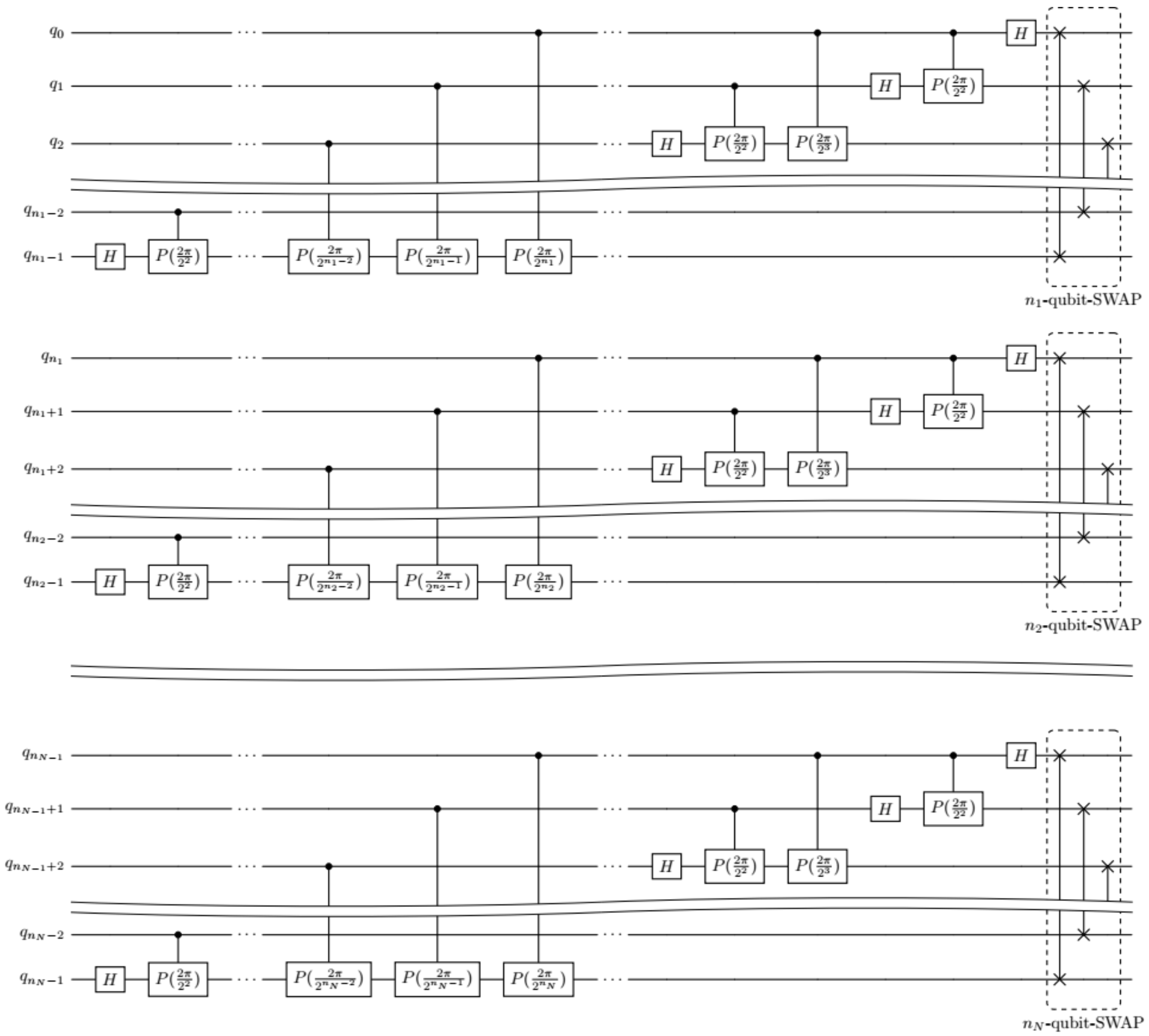

most significant bit (MSB)

Linear Combination of Unitaries (LCU)

A. M. Childs and N. Wiebe, Quantum Information and Computation **12**, No. 11 & 12 (2012)

- expression of an arbitrary matrix A as a linear combination of unitary matrices:

$$A = \sum_{k=0}^{N-1} a_k U_k, \quad a_k \in \mathbb{C},\ U_k^\dagger = U_k^{-1}$$

→ A natural choice for the basis matrices are the tensor products of the 2×2-Pauli matrices $\{\mathbf{1}, X, Y, Z\}$.

- definition of a 'preparation gate' $[PREP(c_0, \dots, c_{N-1})]$ for the state of an ancilla qubit register and a 'selection gate' $[SELECT]$ according to

$$[PREP(\sqrt{a_0}, \dots, \sqrt{a_{N-1}})]|0\rangle_a = \sum_k \frac{\sqrt{a_k}}{\sqrt{\lambda}}|k\rangle_a, \quad \lambda = \sum_k \sqrt{a_k} \cdot (\sqrt{a_k})^* = \sum_k |\sqrt{a_k}|^2 \geq 0$$

$$[SELECT] = \sum_k |k\rangle_a \langle k|_a \otimes U_k$$

$$\Rightarrow \quad [SELECT]|k\rangle_a \otimes |\psi\rangle = |k\rangle_a \otimes U_k|\psi\rangle$$

$$\Rightarrow \underbrace{\langle 0|_a \left[PREP((\sqrt{a_0})^*, \ldots, (\sqrt{a_{N-1}})^*)\right]^\dagger}_{\widehat{=}\ \left(\left[PREP((\sqrt{a_0})^*,\ldots,(\sqrt{a_{N-1}})^*)\right]|0\rangle_a\right)^\dagger} [SELECT] \left[PREP(\sqrt{a_0}, \ldots, \sqrt{a_{N-1}})\right] |0\rangle_a \otimes |\psi\rangle$$

$$= \sum_{k'} \frac{\sqrt{a_{k'}}}{\sqrt{\lambda}} \langle k'|_a [SELECT] \sum_k \frac{\sqrt{a_k}}{\sqrt{\lambda}} |k\rangle_a \otimes |\psi\rangle = \sum_{k'} \sum_k \frac{\sqrt{a_{k'}}\sqrt{a_k}}{\lambda} \underbrace{\langle k'|k\rangle}_{=\delta_{k,k'}} U_k |\psi\rangle = \frac{1}{\lambda} \sum_k a_k U_k |\psi\rangle = \frac{1}{\lambda} A|\psi\rangle$$

→ quantum circuit representation:

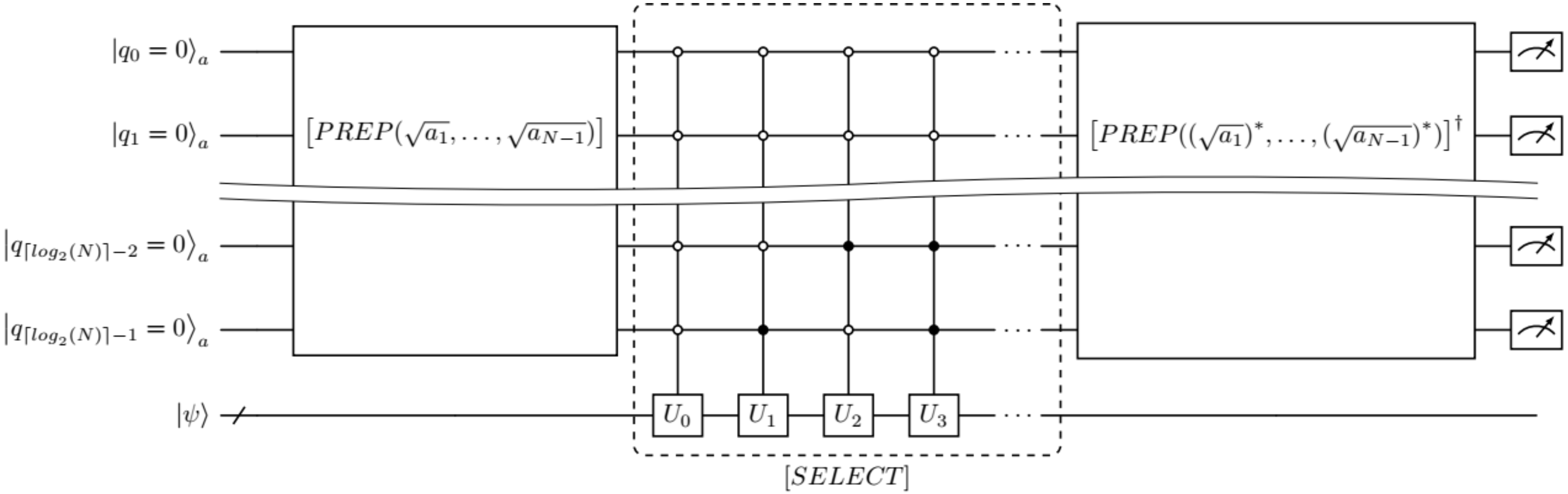

Structure of the Full Quntum Algorithm

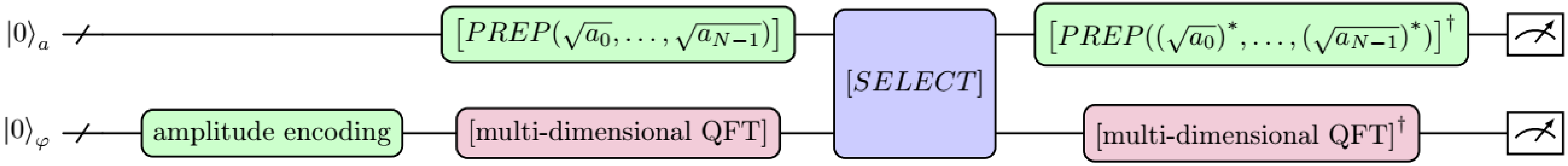

→ functionality verified via implementation and simulation with *IBM Qiskit*

Results from Statevector Calculation

- considered source term $S(x) = \frac{\partial^2}{\partial x^2}\left(e^{-\frac{(x-x_0)^2}{\sigma^2}}\right) \Rightarrow \varphi(x) = e^{-\frac{(x-x_0)^2}{\sigma^2}} + const.$
  with $\sigma = \frac{0.2}{\sqrt{\ln(2)}}$ and $x_0 = 4$

source field → quantum algorithm → **real part** | **imaginary part**

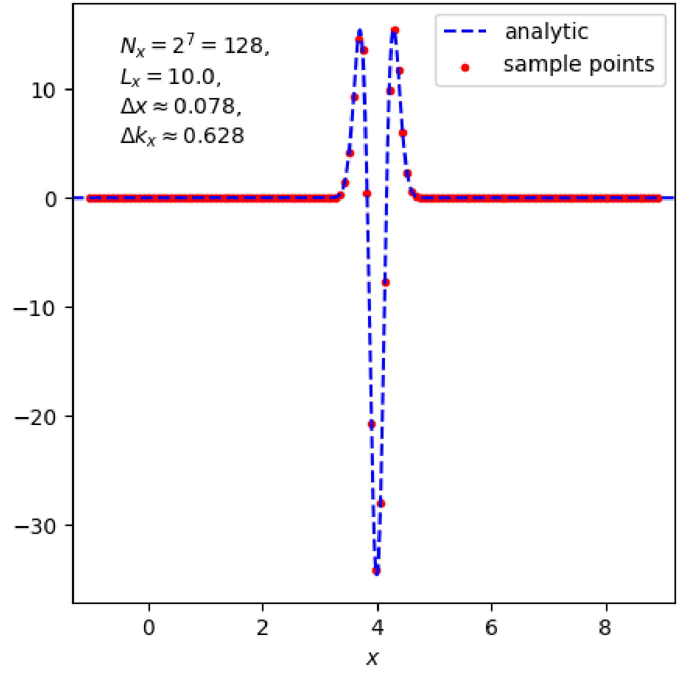

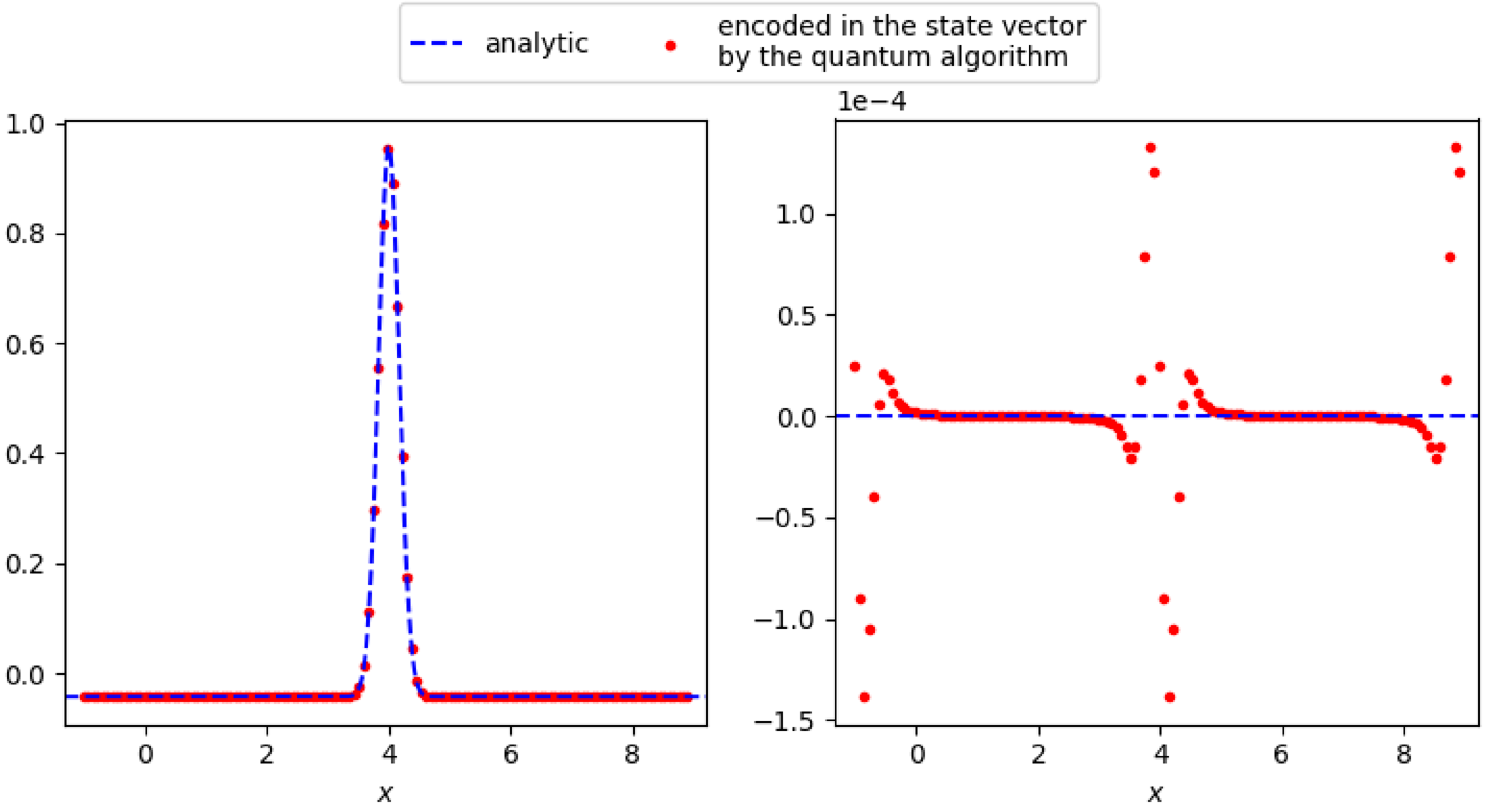

in total 14 qubits

probability for the desired measurement outcome w.r.t. the ancilla qubits ≈ 0.0001

- considered source term $S(x) = e^{-\frac{(x-x_0)^2}{\sigma^2}} \Rightarrow \varphi(x) = \frac{\sigma^2}{2} e^{-\frac{(x-x_0)^2}{\sigma^2}} + \frac{\sigma\sqrt{\pi}}{2}(x-x_0) erf\left(\frac{x-x_0}{\sigma}\right) + const.$
  with $\sigma = \frac{0.2}{\sqrt{\ln(2)}}$ and $x_0 = 4$

source field | quantum algorithm | real part | imaginary part

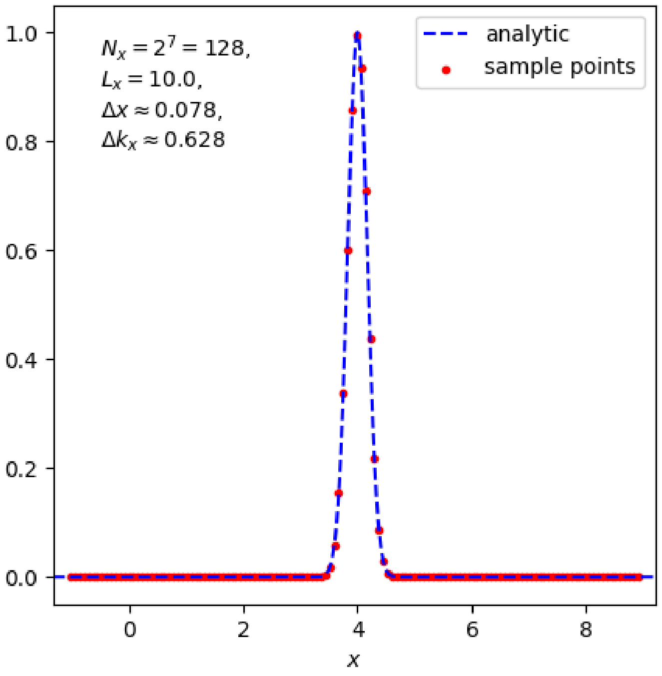

in total 14 qubits

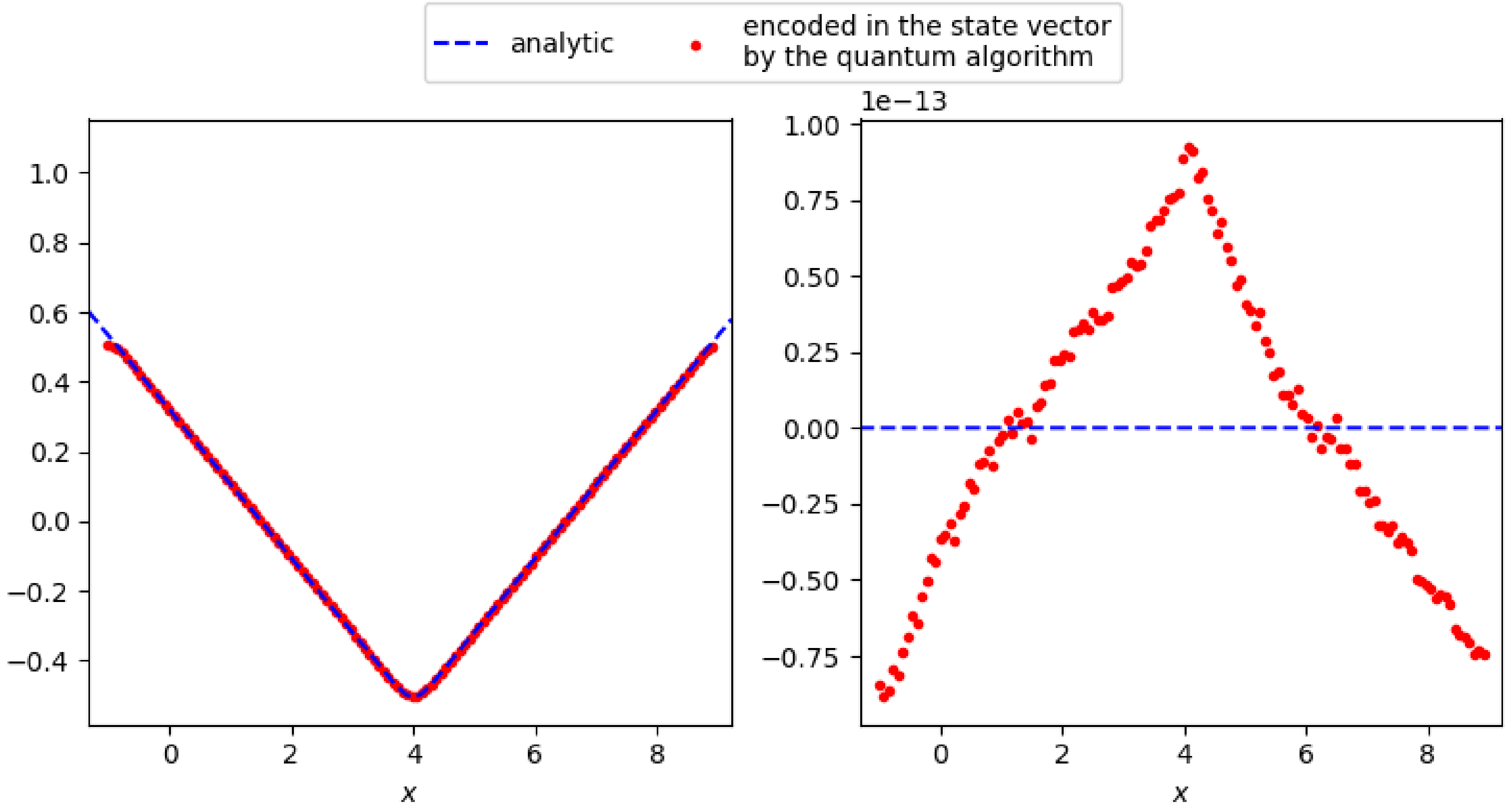

probability for the desired measurement outcome w.r.t. the ancilla qubits ≈ 0.121

- considered source term $S(x,y) = \left[\frac{\partial^2}{\partial x^2} + \frac{\partial^2}{\partial y^2}\right] e^{-\frac{(x-x_0)^2+y^2}{\sigma^2}} \Rightarrow \varphi(x,y) = e^{-\frac{(x-x_0)^2+y^2}{\sigma^2}} + const.$
  with $\sigma = \frac{0.2}{\sqrt{\ln(2)}}$ and $x_0 = 4$

source field | analytic solution | quantum algorithm | real part | imaginary part

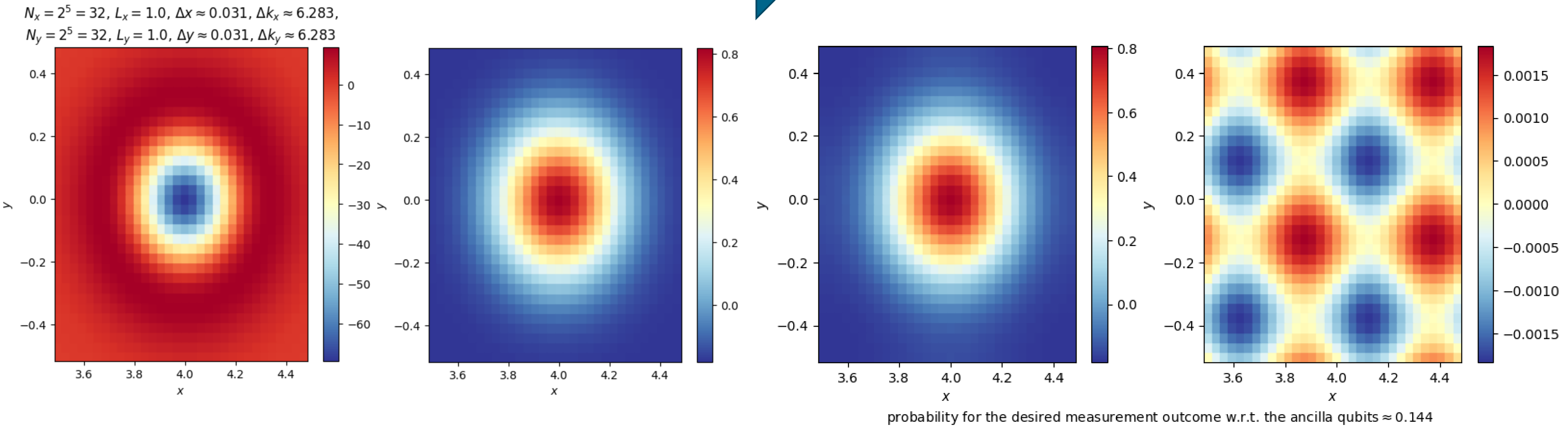

in total 20 qubits

Rough Estimation of Execution Times

- considered so far:
  - QC routines of the presented quantum algorithm
  - quantum algorithm for the LB simulation of a linear advection-diffusion eq. by D. Wawrzyniak et al., Computer Physics Communications **306**, 109373 (2025)

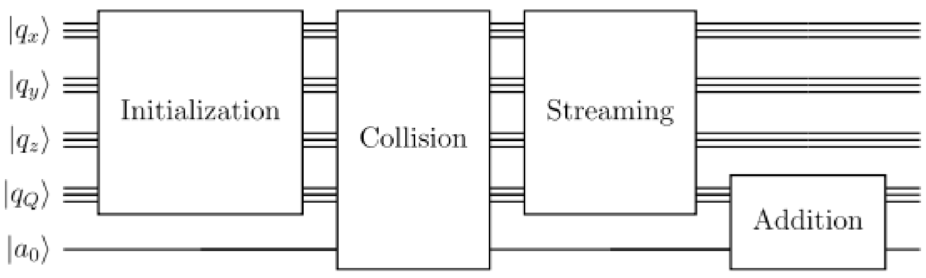

Fig. 1. Quantum circuit with general blocks for the computation of one time step for the Lattice-Boltzmann method in three dimensions.

- done based on the decomposition of the gates in the depicted quantum circuits into native gates according to the procedure in V. V. Shende et al., *IEEE Transactions on Computer-Aided Design of Integrated Circuits and Systems* **25**, 6 (2006)

  and using time scales for superconducting circuits:

1-qubit-gates	50 ns
2-qubit-gates	200 ns
coherence time	100 µs

cf. values in
F. Tennie et al., Nature Reviews Physics (2025);
A. Kandala et al., Phys. Rev. Lett. **127**, 130501 (2021)

Results

		number of native 1-qubit-gates	number of CX-gates
amplitude encoding		$2^{n+1}-2$	$2^{n+1}-2(n+1)$
arbitrary diagonal operator		2^n-1	2^n-2
contributions to the QFT	H-gates	$2n$	0
	CP-gates	$2^{n+1}-n-3$	$2^{n+1}-2(n+1)$
	multi-qubit-SWAP-gate	0	$3\cdot\lfloor\frac{n}{2}\rfloor$

Number of required native gates to realize the listed QC routines for the application to n qubits.

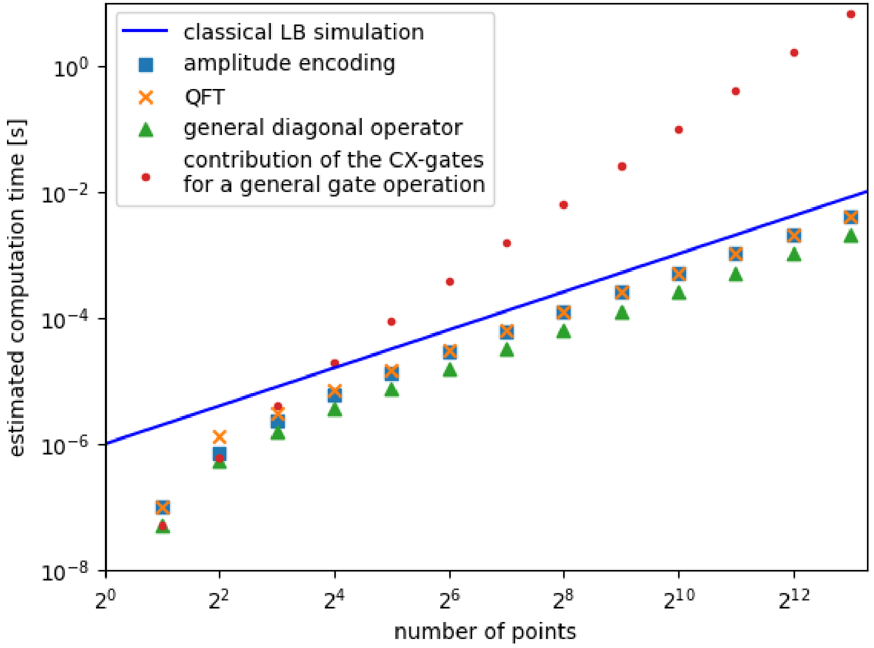

Estimated runtime for some procedures, where the runtimes of the QC routines are referred to one run of the circuits.

	considered grid resolution and stencil	
	300×300, D2Q9	$1000\times1000\times1000$, D3Q27
initialization	0.14 s	437 s
collision	1.68 s	13744 s
streaming	0.05 s	1 s
addition	$2.8\cdot10^{-6}$ s	$3.5\cdot10^{-6}$ s

Estimation of the runtime for one run of the individual steps of the LB quantum algorithm proposed in D. Wawrzyniak et al., Computer Physics Communications **306**, 109373 (2025).

Conclusion

DLR

→ execution of whole quantum algorithms for CAA problems on real hardware seems very challenging (cf. coherence time)

- reference: for a classically implemented LB simulation ≈ **1 μs per grid point and time step**

	considered grid resolution and stencil	
	300 × 300, D2Q9	**1000 × 1000 × 1000, D3Q27**
(a): in total for one run of the quantum algorithm of D. Wawrzyniak et al., Computer Physics Communications **306**, 109373 (2025)	1.87 s	14182 s
(b): classical LB simulation	0.09 s	1000 s
ratio (a) / (b)	20.778	14.182

→ better scaling behavior of such quantum algorithms might be compensated by the need to perform more runs in order to maintain the accuracy of the extraction of the solution values

THANK YOU VERY MUCH FOR YOUR ATTENTION!

Simulation result of a FM-BEM procedure (FMCAS) used at the DLR department ‘Technical Acoustics‘

Imprint

Topic: Potential Directions for the Use of Quantum Computing in CAA

Date: 10 October 2025

Authors: Hans A. Kösel (hans.koesel@dlr.de) and Roland Ewert

Institute: Institute of Aerodynamics and Flow Technology,
German Aerospace Center (DLR),
Lilienthalplatz 7, 38108 Braunschweig, Germany